Tellus (1988), *40A*, 205–219

Intraseasonal fluctuations in low-level meridional winds over the south China Sea and the western Pacific and monsoonal convection over Indonesia and northern Australia*

By W. L. SUMATHIPALA and T. MURAKAMI, *Department of Meteorology, University of Hawaii at Manoa, 2525 Correa Road, Honolulu, Hawaii 96822, USA*

(Manuscript received 9 February; in final form 3 August 1987)

ABSTRACT

Outgoing long-wave radiation (OLR), objectively analyzed daily winds (u, v) and geopotential height data for 5 northern winters are used to study the relationship between low-level equatorward (meridional) winds and tropical convection on the 30–60 day time scale. The general tendency of equatorial 30–60 day OLR perturbations is to propagate eastward. Occasionally, these perturbations exhibit irregular movement. This study is limited to the periods when the eastward propagation is clearly defined.

Correlation maps indicate that the low-frequency modes are of global-scale character with zonal wavenumber one. The low-level 30–60 day northerly wind along the eastern edge of the Siberian high (anomaly) does not contribute to convection and monsoon activity in the Indonesian–northern Australian region. However, 30–60 day northeasterly flows of subtropical Pacific origin play a significant rôle in monsoon activity. An active monsoon condition with strong upper-level southerly outflow from the monsoon region and an intense westerly jet near Japan, is observed approximately 10 days prior to the maximum low-level northerly currents from Siberia.

Fluctuations with periods less than 30 days are considered as transient disturbances. The square of transient meridional winds shows pronounced spectral peaks in the 30–60 day period range. This is associated with an amplitude modulation of synoptic-scale transient disturbances, which is most pronounced in both the NH and SH extratropics. Perhaps, transient disturbances, as a group, can make a contribution toward the enhancement and/or maintenance of extratropical low-frequency perturbations.

1. Introduction

Based on spectral analysis of rawinsonde data at Canton Island, Madden and Julian (1971) detected a low-frequency mode with a period range of 40–50 days. Since then many investigators have reported on the existence of long-period oscillations for all meteorological parameters. Observational studies confirm that these perturbations are on a global scale with a zonal wavenumber one and an eastward speed of 8° longitude per day (Krishnamurti et al., 1985; Lorenc, 1984). However, these global-scale waves tend to amplify while passing through the eastern hemisphere monsoon domain (Murakami et al., 1986). Theoretical studies aimed at identifying the origin of these waves indicate that they can be internally enhanced by large-scale convection (Hayashi and Sumi, 1986; Chang, 1977). Since no external forcing was included in their theoretical models, these low-frequency waves can be considered as a free mode in the equatorial region.

By examining 28–72 day filtered tropical OLR and global 250 mb streamfunctions for 10

* Contribution no. 87-10, Department of Meteorology, University of Hawaii, USA.

winters, Weickmann et al. (1985) found a strong response in the 250 mb streamfunction fields over the subtropical and middle latitudes, implying a tropical-midlatitudes interaction on this time scale. The lateral coupling due to 30–50 day modes during the 1978–1979 northern winter was detailed by Quah (1984). Krishnamurti and Gadgil (1985) detected a strong signal of low-frequency oscillations in high-latitude regions. Recently, Lau and Phillips (1986) found significant tropical–extratropical teleconnections with regard to the eastward propagation of low-frequency OLR perturbations across the Indian Ocean and the western equatorial Pacific during winter.

Several investigators have indicated that transient northerly surges over the south China Sea during the northern hemisphere winter* can enhance synoptic-scale equatorial convection (Ramage, 1971; Chang and Lau, 1982; Lim and Chang, 1981). Murakami (1987a) showed evidence of 30–60 day southerly flows from the SH midlatitudes causing convection over the Asiatic monsoon domain during summer. These equatorward flows on the 30–60 day time scale can be considered as an external forcing on convection in the NH monsoon domain. Since the amplification of low-frequency modes is unique to the eastern hemisphere, 30–60 day oscillations can be considered as forced waves localized in the monsoon region.

In this paper, we examine the relationship between 30–60 day northerly flows in the NH midlatitudes upon the convective activity in the SH monsoon region where low-frequency modes are dominant. Further, we look at the relation between transient eddies and the low-frequency perturbations during winter.

2. Data and computational procedures

This study utilized daily winds (u, v) at two levels (200 and 850 mb) and geopotential heights (Φ) data at 850 mb during the 5 winters (1 November–31 March) of 1979 to 1984. These data were extracted from the objectively analyzed data set prepared by the European Centre for Medium Range Weather Forecasts (ECMWF) over the global region between 65° N and 65° S at a 2.5° latitude/longitude resolution. Daily outgoing long-wave radiation (OLR) data obtained from polar orbiting satellites at a 2.5° latitude/longitude resolution for a tropical belt between 45° N and 45° S were also used.

By applying harmonic analysis to daily data, the yearly and half-yearly cycles were computed. The sum of these two cycles is largely associated with the seasonal cycle. Introducing angle braces $\langle\ \rangle$ to represent the seasonal cycle including the annual mean and a prime to define the departure from it; u for example, can be expressed as

$$u = \langle u \rangle + u'. \tag{1}$$

Hence, u' represents the intraseasonal component of u. A band-pass filter is then applied to u', utilizing the procedure outlined by M. Murakami (1979), to extract 30–60 day filtered data. Using the notation $(\tilde{\ })$ to represent these filtered data, we further separated u' into two components as follows:

$$u' = \tilde{u} + u^*, \tag{2}$$

where, u^* represents the transient variations with periods shorter than 30 days.

The general tendency of 30–60 day perturbations is to propagate eastward especially over the equatorial Indian Ocean–western Pacific region (Murakami et al., 1986). Sporadically, these perturbations exhibit irregular movement or even westward propagation. Fig. 1 depicts time–longitude sections of $\widetilde{OLR}$ for 5 winters average over a latitude belt 0°–10°S from 50°E to 180°. There are periods when the eastward propagation is clearly defined; such as, 20 November–21 December 1979; 29 January–31 March 1980; 19 February–31 March 1981; 17 November 1981–8 February 1982; 10 November 1982–8 February 1983; 1 November–10 December 1983; 28 February–31 March 1984. These 384 days of eastward propagation are designated "E" phases and are indicated by heavy arrows in Fig. 1. The periods of irregular movement are signified as "NE" phases, and total 371 days.

* For brevity, the term "northern hemisphere" will rarely be used when identifying the seasons. Thus, the term "winter" refers either to the northern hemisphere (NH) winter or to the southern hemisphere (SH) summer, while the term "summer" is used either for the NH summer or for the SH winter.

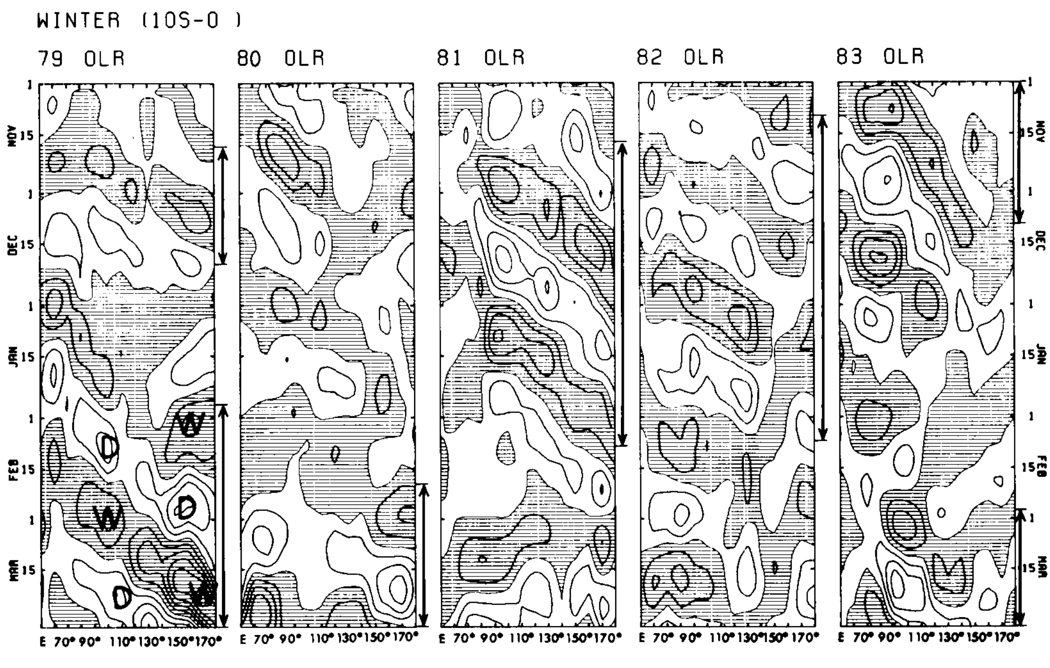

Fig. 1. Time–longitude sections of 30–60 day filtered OL̃R averaged between the equator and 10°S from 50°E to the date line for 5 winters (1979–1984). Intervals are 10 W m^{-2} with negative anomaly hatched. W (D) denotes peak wet (dry) periods. Heavy arrows indicate E phases with systematic eastward propagation.

Amplitude of the OL̃R perturbations during E phase is large in comparison to NE phase (Fig. 1). Large amplitude is indicative of strong convective activity in the monsoon domain which supplies substantial amounts of energy to the 30–60 day mode during E phase. Since the 30–60 day signal is fully established during E phase, we anticipate enhanced interactions between the tropical and midlatitude regions. Lau and Lau (1986) showed that eastward propagation of low-frequency modes cannot be seen at all times in the GFDL record. They discussed some of the statistical and dynamical aspects of model generated low-frequency modes only during periods of regular eastward propagation. The present paper is concerned with observed atmospheric low-frequency modes only during the E phase. The reader is directed to Murakami's (1987b) paper for the nature of low-frequency oscillations during the NE phase in winter. The basic difference between the present paper and Murakami's paper is, among other things, the use of different analysis techniques. Murakami's paper was based on a composite technique, while the present paper uses a correlation method. The agreement between the two methods lends creditability to the use of either technique for appropriately describing the behavior of low-frequency modes. To avoid repetition, we deleted the NE phases in the present paper.

Fig. 1 indicates an equatorial dipole feature, as noted by previous investigators (Lau and Chan, 1985; Murakami et al., 1986), with one leg over the equatorial Indian Ocean around 100°E and the other leg in the western Pacific around 160°E. For example, on 20 March 1980, the equatorial Indian Ocean is characterized by dry conditions (denoted by D) while the western Pacific experiences wet conditions (designated by W). Conversely, when the equatorial Indian Ocean is wet, the western Pacific is dry. This feature is also noticeable during the E phases of any year.

Since the aim of this study is to investigate midlatitude–tropical interactions using one point correlation maps with respect to a time series of 850 mb $\tilde{\Phi}$ at a reference area, it is important to determine the statistical significance of these correlation patterns. Following the same procedure as used by Lau and Phillips (1986), the local correlation coefficients greater (less) than 0.3 (−0.3) are found to be locally significant at the 95% confidence level. The areal percentage that surpasses the local 95% confidence level is denoted as "LS". In order for a correlation map to be globally significant, LS should exceed a critical value. The method for testing the global significance was reported by Lau and Phillips (1986), and Shrestha and Murakami (1988). The reader is directed to these papers for a complete description of the statistical test. The globally significant criterion, which was determined from a Monte Carlo experiment, is indicated as "GS" in each correlation map. If LS for a particular map is greater than GS, the correlation pattern is considered to be globally significant. As will be shown later, most of the correlation maps are globally significant at the 95% confidence level.

3. Correlation patterns for transient disturbances

Using areal average 850 mb transient geopotential heights Φ* over the east China Sea region

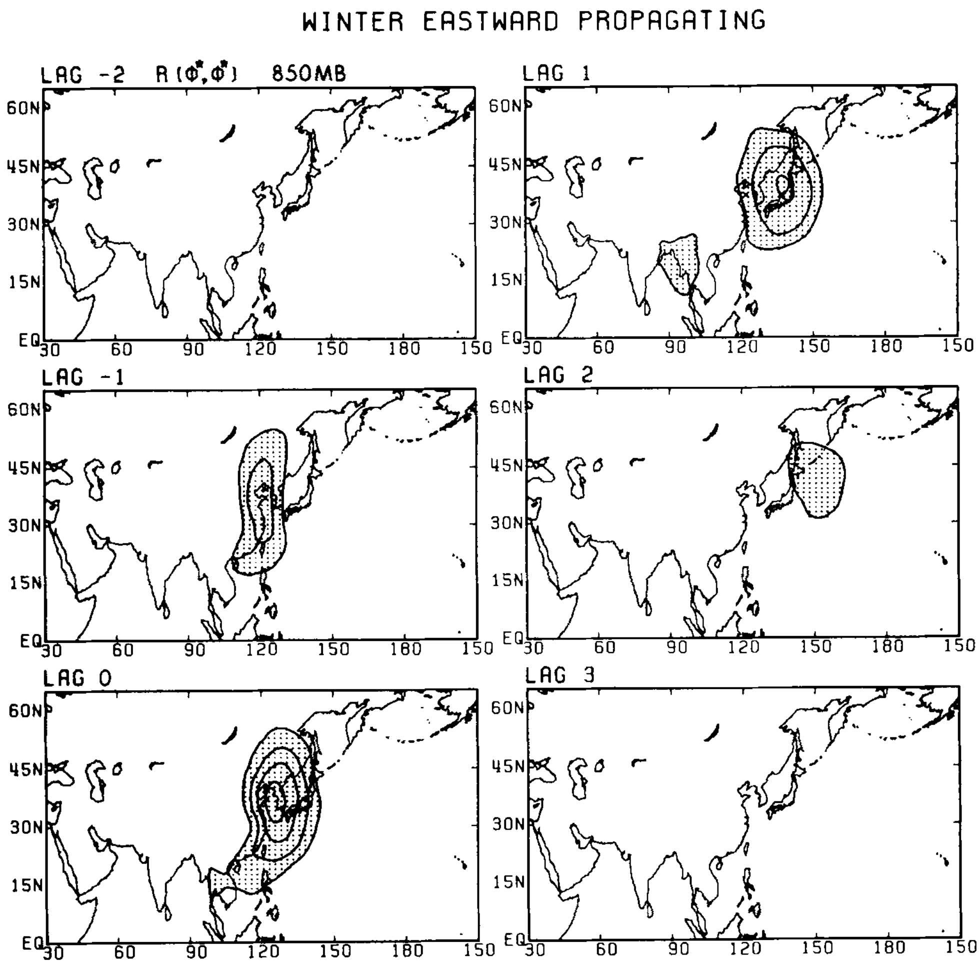

Fig. 2. Lag correlation patterns of transient geopotential height Φ* at 850 mb with reference to the average Φ* over the east China Sea area (30°–40°N, 120°–130°E) for lag −2, −1, ..., and +3. Intervals are 0.2 and areas of correlation coefficient greater than 0.3 are stippled.

(30°–40° N, 120°–130° E) as the reference time series, lag correlation coefficients were computed for 850 mb Φ^* at every grid point. This reference area lies in the path of severe cold outbreaks from the Siberian high-pressure region. In Fig. 2, shading indicates regions where the local correlation coefficient is significant at the 95% confidence level. Although the lag correlation was computed for the global domain, it exceeds the confidence level only in the immediate vicinity of the reference area. Thus, Fig. 2 depicts the regional synoptics of transient disturbances. An elongated north–south structure at lag -1 day may indicate the extent of a cold surge from Siberia. At lag 0, correlation is maximum ($+1$) at the reference area with values greater than $+0.3$ extending southward to the south China Sea. The center of this synoptic disturbance shifts from the east coast of China (35° N, 120° E) at lag -1 to east of Japan (43° N, 150° E) at lag $+2$ with an eastward phase speed of about 10 m s^{-1} and an approximate wavelength of 6000 km. This pattern exemplifies the nature of transient northerly surges associated with midlatitude baroclinic wave disturbances. Correlation maps with other key reference areas show similar local synoptics (not shown).

Section 4 investigates the relationship between low-level equatorward winds from the NH midlatitudes and convection over the SH monsoon region on the 30–60 day time scale. The equatorward $\tilde{v}$ winds appear to exert a strong measure of control upon the enhancement of planetary-scale low-frequency modes over the global tropics.

4. Correlation patterns for low-frequency perturbations at 850 mb

In order to study the nature of 30–60 day $\tilde{\Phi}$ perturbations, lag correlation coefficients were computed with reference to $\tilde{\Phi}$ variations over the east China Sea (30°–40° N, 120°–130° E). These correlation patterns show that 30–60 day $\tilde{\Phi}$ perturbations are of global-scale character (Fig. 3). As discussed in Section 2, since LS > GS for all four correlation maps (3a, b, c and d), these patterns are globally significant at the 95% confidence level.

The lag 0 map (Fig. 3c) with the maximum correlation (1.0) at the reference point reveals a marked zone of greater than $+0.3$ values extending over China through India to South Africa. Similarly, large areas of negative (< -0.3) correlation are found east of Australia, the eastern north Pacific and the north Atlantic. These correlation patterns are characterized by zonal wavenumber one with a distinct southwest–northeast tilt. Here, note that the lag 0 correlation map actually defines two anomalous patterns since 850 mb $\tilde{\Phi}$ at the reference point may be either positive or negative. For brevity, a description of the correlation map is given for the case when 850 mb $\tilde{\Phi}$ is positive. Thus, regions of positive (negative) correlation in Fig. 3c correspond to anomalous high (low) pressure cells. The most important indication in the lag 0 correlation map is the possible existence of strong pressure gradient along the eastern edge of an anomalous high-pressure cell located at the reference point. Associated with this strong pressure gradient are prominent low-level northerlies carrying continental cold air from Siberia toward the equator (refer to heavy asterisks in Fig. 3c). These 30–60 day northerlies, which are of Siberian origin, are hereafter signified as "NS" northerlies. At lag 0, note a zonally oriented band of anomalous low pressure (negative correlation) stretching over the western south Pacific east of Australia. Perhaps, this is indicative of above normal monsoon activity over this region. In Fig. 3b for lag -5, the northeastern Australia–New Guinea region is dominated by an anomalous trough, probably reflecting an active phase of the SH summer monsoon. Further north of this anomalous trough are prominent northeasterlies that are associated with a strong pressure gradient over the western equatorial north Pacific (refer to heavy dots in Fig. 3b). These northeasterlies, which are of Pacific origin, are denoted as "NP" northerlies. The NP northerlies appear to converge in the SH monsoon region and contribute to the enhancement of equatorial convection. At day -5, the NS northerlies from Siberia contribute little, if any, to the SH monsoon activity on the 30–60 day time scale. This can be more firmly substantiated from an inspection of Fig. 3a for lag -10, which depicts the presence of NS northerlies only over central Siberia. These NS northerlies prevail east and southeast of an anomalous high-pressure cell

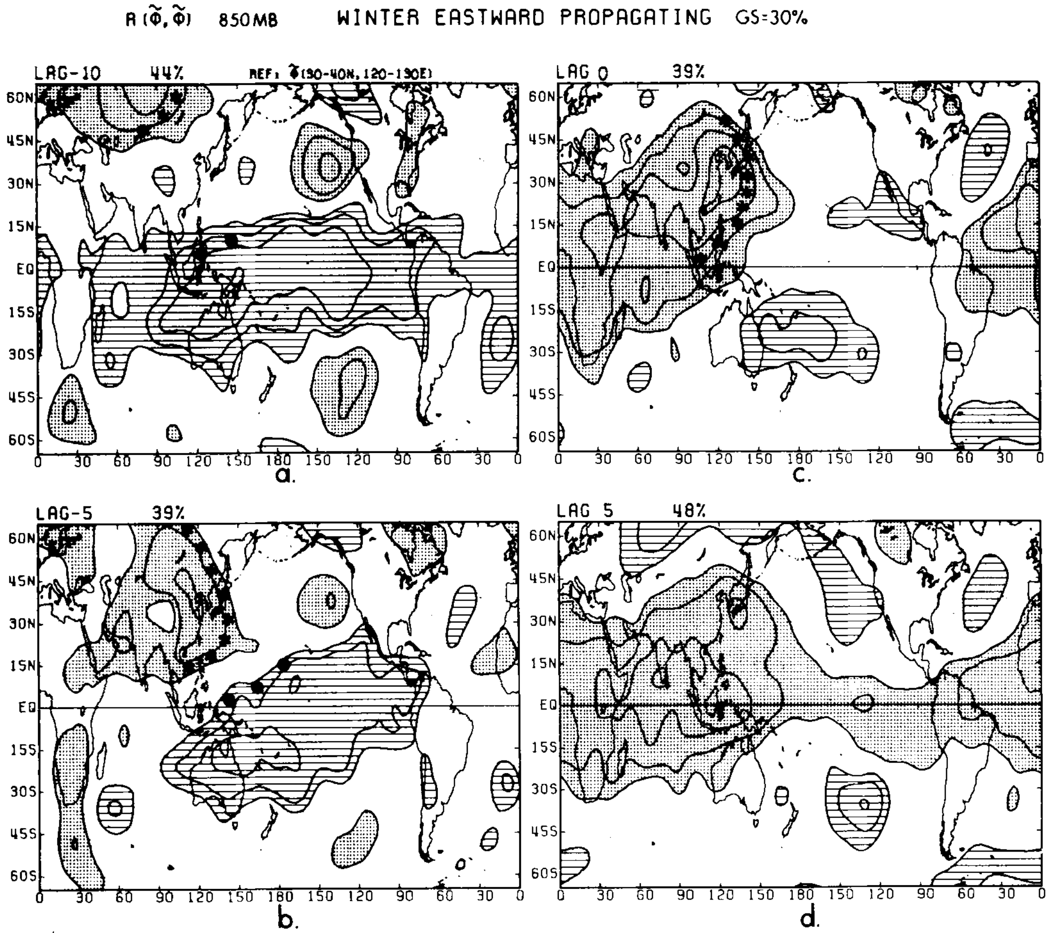

Fig. 3. Lag correlation of 30–60 day filtered geopotential height $\tilde{\Phi}$ at 850 mb with reference to the area average $\tilde{\Phi}$ over the east China Sea area (30°–40° N, 120°–130° E) for lag −10, −5, 0, and +5 days. Intervals are 0.2 and regions of correlation coefficient greater (less) than 0.3 (−0.3) are stippled (hatched). Heavy dots (asterisks) denote an approximate route of NP (NS)-type 30–60 day northerlies. Local significance value (LS) shown at the top of each correlation map is to be compared with global significance value (GS) at the top-right corner of this diagram.

centered at 65° N, 80° E. Between day −10 and 0, the high-pressure cell moves eastward across Siberia, reaching the reference point at day 0. Yet another feature of interest in Fig. 3a for lag −10 is the tendency for NP northerlies to converge into the SH monsoon trough (anomaly). At this time, the monsoon trough is abnormally intensified over the SH monsoon region (Indonesia–northern Australia–New Guinea).

As far as the authors know, no investigator has yet examined anomalous northerlies from Siberia on the 30–60 day time scale. Anomalous northerlies of subtropical Pacific origin have never drawn the attention of monsoon meteorologists.

To further confirm the existence of NS and NP northerlies, lag correlations $R(\tilde{\Phi}, \tilde{v})$ were computed for global $\tilde{v}$ at 850 mb using the same reference (850 mb $\tilde{\Phi}$ at 30°–40° N, 120°–130° E). Correlation patterns for lag −10, lag −5, and lag 0 day are globally significant at 95% confidence level (LS > GS), while the lag 5-day map is not globally significant (Fig. 4). Yet this correlation map exhibits some interesting synoptics that pass

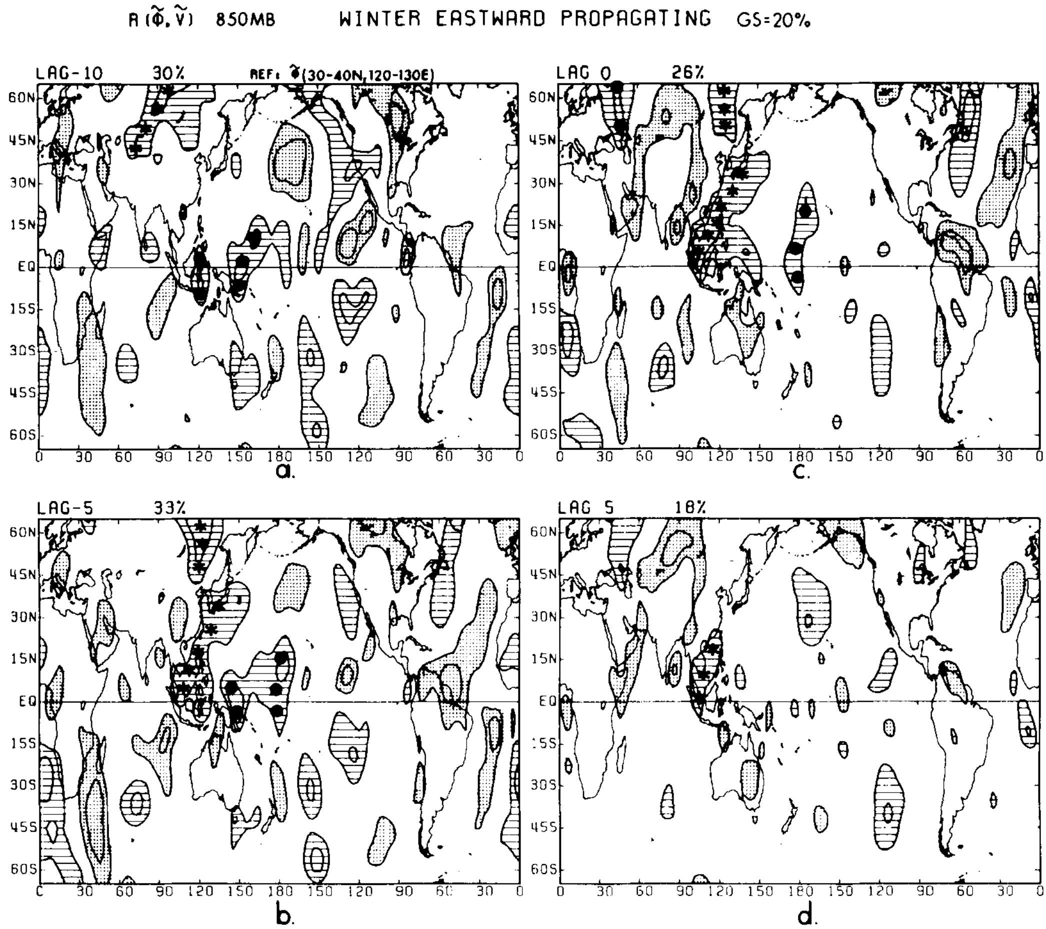

Fig. 4. As in Fig. 3, except for meridional wind $\tilde{v}$ at 850 mb.

the local 95% confidence level. The lag −10 day pattern shows a distinct separation of NS from NP northerlies. At this time, the monsoon over Indonesia and northern Australia is active and the NP northerlies cross the equator and activate convection in the monsoon area, while NS northerlies are now limited to north of 45°N. By lag −5 day as the low-pressure area (monsoon trough) shifts eastward NP northerlies move along with it (Fig. 4b). These NP northerlies still feed into the SH convective region at day −5. Concurrently, NS northerlies move over eastern Siberia as well as extending southward to the tropics. On lag 0 day, the NP northerlies are over the equatorial central Pacific and are completely separated from NS northerlies which penetrate into the equatorial latitudes across the south China Sea. However, the effect of these NS northerlies on convective activity in and around the monsoon trough east of Australia is minimal (Fig. 3c).

Next, 850 mb $\tilde{\Phi}$ at the same reference area was correlated with 850 mb $\tilde{u}$ at every grid point in the global domain (refer to Fig. 5). O$\tilde{L}$R values at every grid point from 45°S to 45°N were also correlated with the same base time series of 850 mb $\tilde{\Phi}$ (see Fig. 6). All maps in Figs. 5 and 6 surpass the global significance at the 95% confidence level (LS > GS). In Fig. 5a for lag −10 day, NS northerlies over central Siberia are associated with easterlies. Strong westerlies (positive correlation) over Indonesia signify the

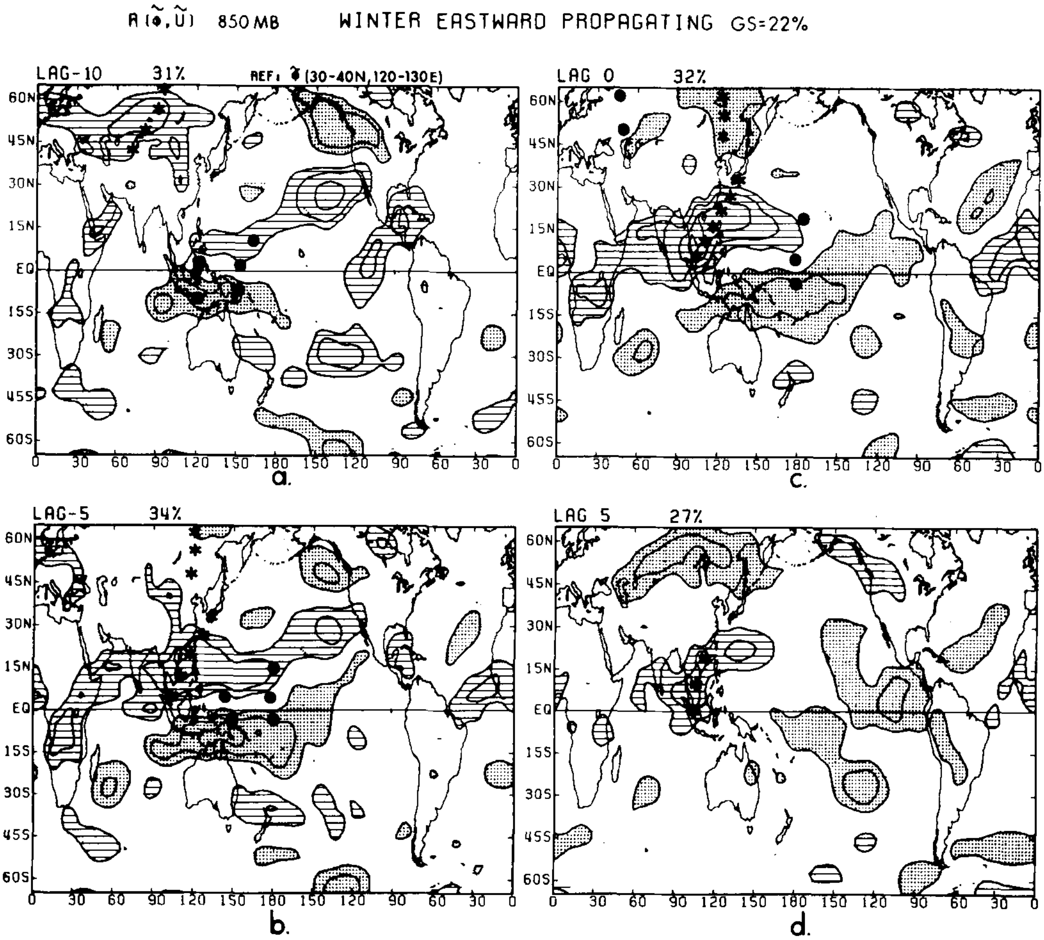

Fig. 5. As in Fig. 3, except for zonal wind $\tilde{u}$ at 850 mb.

active monsoon condition. In the equatorial western Pacific, NP northerlies feed into the monsoon westerlies. At this time convection is strongest ($\widetilde{\mathrm{OLR}} < 0$) over the Indonesia–northern Australia–New Guinea area (Fig. 6a). This reconfirms our previous statement that NP northerlies control monsoon activity. Recall that NS northerlies are weak and limited to central Siberia at lag -10 day.

At lag -5 day, NS northerlies become pronounced as the easterlies (anomaly) increase in the south China Sea area (Fig. 5b). Regions of strong monsoon westerlies and convection ($\widetilde{\mathrm{OLR}} < 0$) move eastward to northeast of Australia (Fig. 6b). Also evident in the same diagram is an organized area of positive correlation in $\widetilde{\mathrm{OLR}}$ perturbations over the Indian Ocean around 15°S, 90°E. This corresponds to the western (dry) branch of the dipole feature as observed by Lau and Chan (1985) and Murakami et al. (1986). It is interesting to note that this dipole feature becomes most prominent 5 days after active monsoon conditions over Indonesia and northern Australia.

At lag 0 day, an anomalous westerly region shifts further east in the SH tropics while the area of easterly anomaly moves westward in the NH tropics (Fig. 5c). Convection is most prominent over the central south Pacific where the south Pacific convergence zone appears to be most

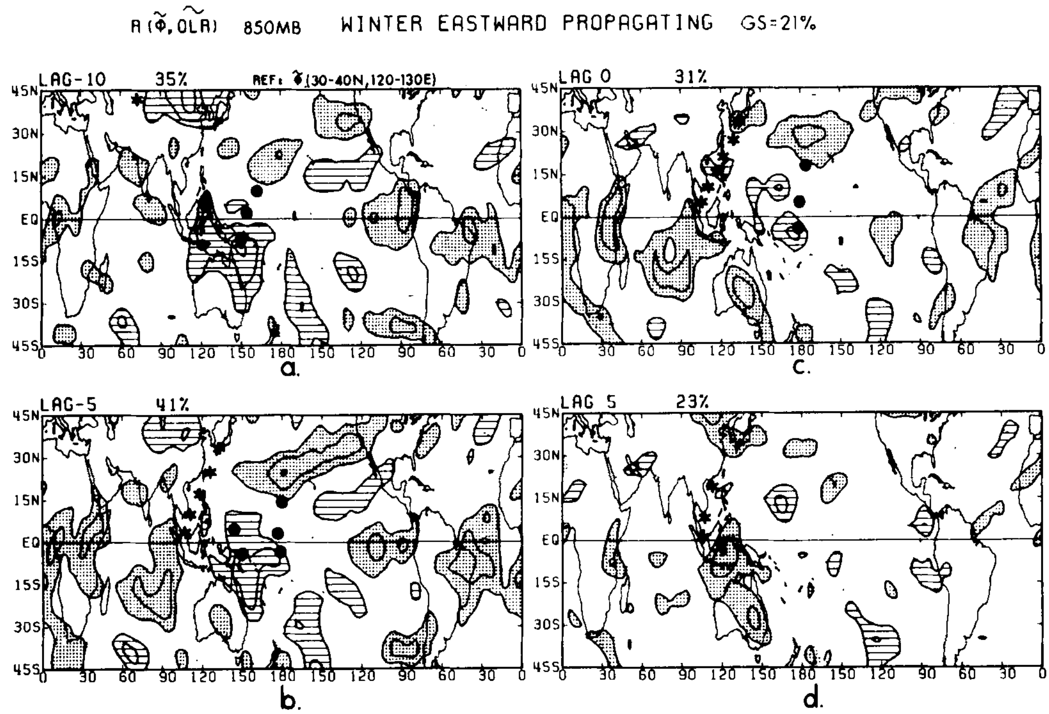

Fig. 6. As in Fig. 3, except for $\widetilde{OLR}$.

pronounced (Fig. 6c). This convective activity near the date line appears to be a direct response to NP northerlies from the equatorial north Pacific which converge into regions of monsoon westerlies in the central south Pacific (Fig. 5c). At lag +5 day, no monsoonal westerlies exist (Fig. 5d) and $\widetilde{OLR}$ indicates a positive correlation (Fig. 6d) over the majority of the monsoon domain. This feature is similar to the break monsoon condition over the Indonesia–northern Australia region.

We have thus far shown lag correlations maps for lags −10 to +5 day only, which cover less than a half cycle of low-frequency (30–60 day) oscillations with an average period of 45 days. The lag +10 day correlation map is nearly identical, except for a change of sign, to that for lag −10 day. At lag +10 day, $\widetilde{OLR}$ becomes positive (below normal convection) over the Indonesia–northern Australia–New Guinea region (Fig. 6a). Associated with this are above normal $\tilde{\Phi}$ (Fig. 3a) and anomalous $\tilde{u}$ easterlies (Fig. 5a) over the same region. Interestingly, convection ($\widetilde{OLR} < 0$) begins to intensify over the Indian Ocean at lag +10 day. Convective regions then propagate eastward, while intensifying substantially, across the Indian Ocean* between lags +15 and +20 day (refer to Figs. 6b and c). At lag +20 day, the Siberian high is depressed well below normal ($\tilde{\Phi} < 0$) with southerly $\tilde{v}$ (Figs. 3a, 4a). Regions of active convection eventually reach the Indonesia–northern Australia–New Guinea area by lag +30 day (see the lag −10 day correlation map for $\widetilde{OLR}$ in Fig. 6a). This completes one cycle of low-frequency (30–60 day) oscillations during winter.

* Lag correlation maps constructed with reference to 850 mb $\tilde{\Phi}$ over central Siberia (5°N, 100°E) indicate strong northerlies flowing along the western periphery of the Tibetan Plateau. These northerlies eventually reach the Arabian Sea and the equatorial Indian Ocean where convection becomes more pronounced than normal. Refer also to Figs. 7 and 8 of Murakami (1987b) for the relationship between the northerlies of central Siberia origin and equatorial convection over the Indian Ocean.

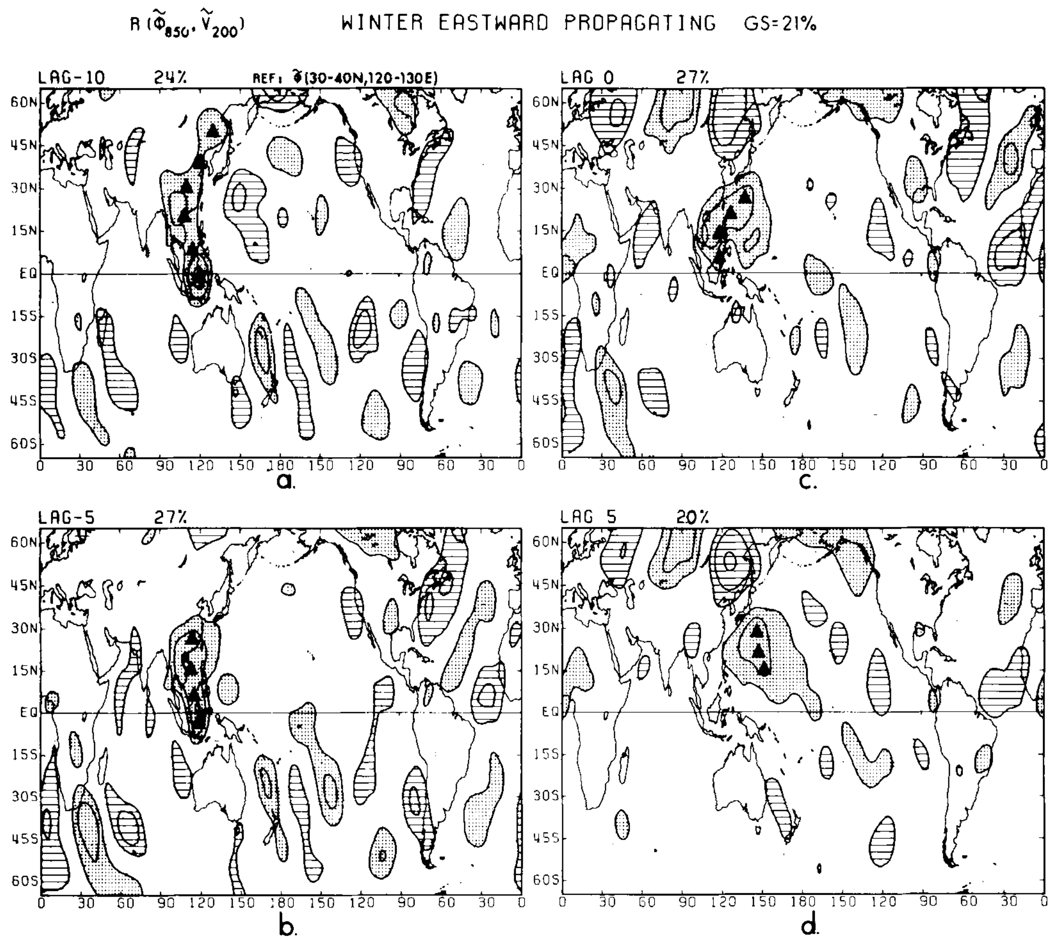

Fig. 7. As in Fig. 3, except for meridional wind $\tilde{v}$ at 200 mb. Heavy triangles indicate the approximate route of NS′ 30–60 day southerlies.

5. Correlation patterns for low-frequency perturbations at 200 mb

Large-scale deep convection in the equatorial region certainly affects the upper tropospheric flow patterns. An attempt is then made to study the 200 mb $\tilde{u}$ and $\tilde{v}$ fields using similar one point correlation maps. Here again, 850 mb $\tilde{\Phi}$ fluctuations at the same reference point (east China Sea) were used as the base time series.

Lag +5 day map for 200 mb $\tilde{v}$ is not globally significant (LS < GS) at the 95% significance level (Fig. 7d), while all lag correlation maps for 200 mb $\tilde{u}$ are globally significant (Figs. 8a to 8d).

Of particular interest in lag −10 day map (Fig. 7a) is the predominant southerlies (positive correlation) over the Far East along about the 120°E meridian. These anomalous southerlies originate in the monsoon of Indonesia–Australia and extend northward through the south China Sea to Siberia. These southerlies are designated an NS′ southerlies* and are denoted by heavy triangles

* Recall that at 850 mb on lag −10 day, NS northerlies over central Siberia are limited to 45°N latitude and are quite weak. The NS northerlies from Siberia become strongest at day 0, i.e., 10 days after the occurrence of strongest NS′ southerlies at 200 mb. Also note that the NP northerlies of Pacific origin are primarily responsible for the enhancement of monsoonal convections over the Indonesia–northern Australia–New Guinea region at lag −10 day.

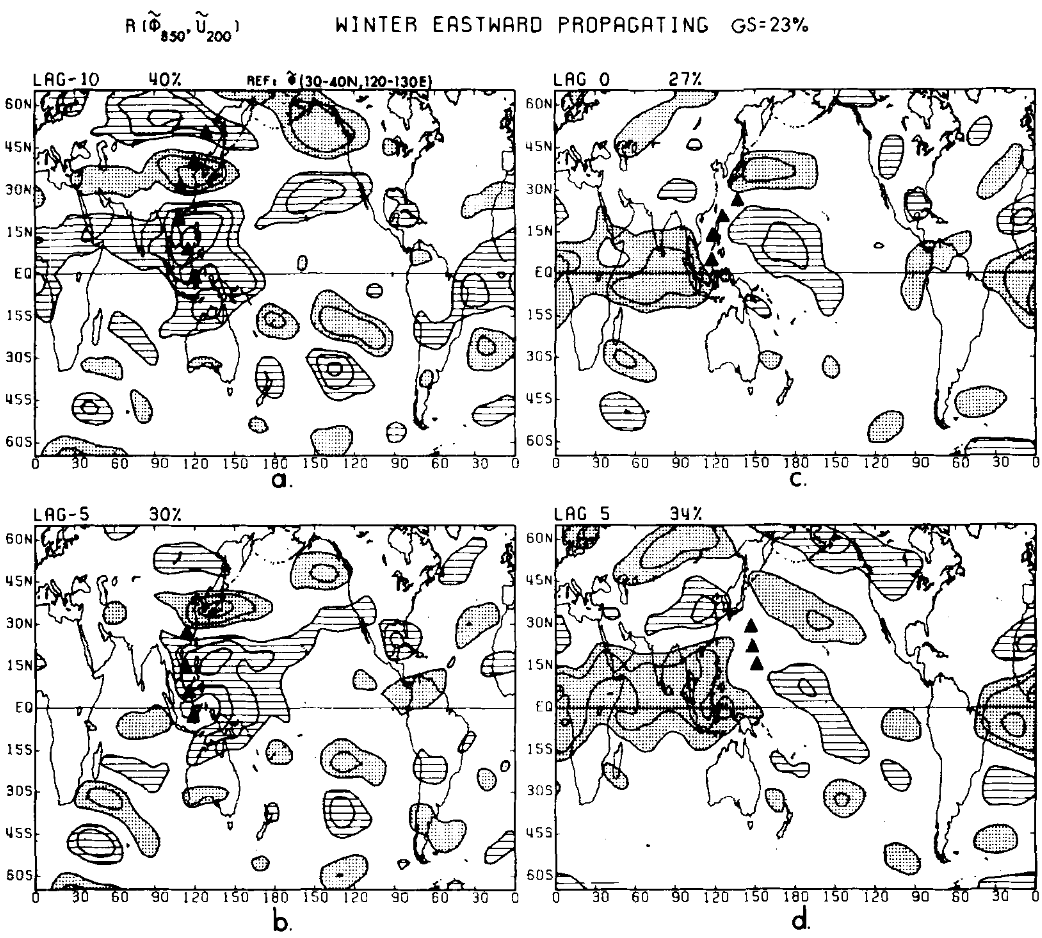

Fig. 8. As in Fig. 3, except for zonal wind $\tilde{u}$ at 200 mb.

in Fig. 7. In Fig. 8a for lag −10 day, strong NS′ southerlies from the monsoon region tend to intensify the westerly jet stream ($\tilde{u} > 0$) over Japan. NS′ southerlies are also distinct at lag −5 day correlation pattern (Fig. 7b). At lag 0 day NS′ southerlies are strong south of Japan. These upper-level NS′ southerlies overlay the low-level NS northerlies (Fig. 4b), implying an intense and deep local Hadley circulation along about 120°E at day 0.

The 200 mb $\tilde{u}$ correlation maps exhibit in phase character with the 850 mb $\tilde{u}$ correlation maps in the NH midlatitudes poleward of about 45°N. Namely, the $\tilde{u}$ perturbations are barotropic in the vertical. Similar barotropic feature is also evident between the 850 and 200 mb $\tilde{v}$ correlation fields over the NH midlatitude region. In comparison, over the equatorial region the correlation patterns are out of phase between the two levels, indicating a baroclinic structure in the vertical.

At lag −10 day, associated with equatorial convection over the monsoon region are two upper-level anticyclonic systems located over central Australia and Taiwan, respectively (not shown). Easterlies are strong between these two anticyclonic systems (Fig. 8a). This feature is consistent with model experiment results (Gill, 1980) as well as observational evidence (Murakami et al., 1986). By lag −5 day equatorial easterlies, the westerly jet stream near Japan, and the equatorial convective region all shift eastward. The lag 0 day map indicates further eastward movement of easterlies across the western Pacific, as well as the westerly jet stream across Japan.

As previously mentioned, all correlation patterns discussed above are produced with the reference area 30°–40°N, 120°–130°E. These one-point correlation patterns were compared with composite maps produced with reference to equatorial OĽR perturbations (Murakami, 1987b) and the agreement was exceptionally high. This confirms the credibility of the computed correlation patterns presented in this paper.

6. Relationship between transient eddies and low-frequency perturbations

By definition of eq. (2), there is no direct correlation between transient eddies and 30–60 day oscillations. Nevertheless, it is possible that transient eddies can interact (correlate) with low-frequency perturbations via an amplitude modulation of the transient eddies. During the SH summer, the preferred area for maximum equatorward penetration of midlatitudinal transient disturbances is the west coast of Australia (Ramage, 1984). Therefore we selected an area

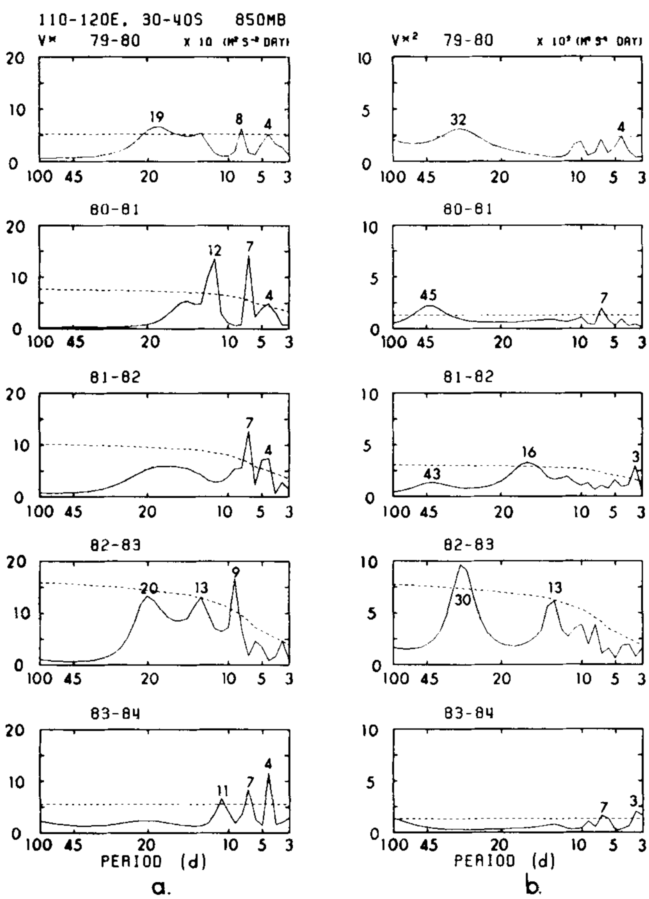

Fig. 9. (a) Power spectra ($m^2\ s^{-2}\ day^{-1}$) for daily transient v^*. (b) Power spectra ($m^4\ s^{-4}\ day^{-2}$) for v^{*2}. Spectra for both (a) and (b) is over the western coastal region of Australia (30°–40°S, 110°–120°E). Dashed line is for the 95% significance level of power spectra.

(30°–40°S, 110°–120°E) in the eastern Indian Ocean to study the relationship between transient eddies and the low-frequency perturbations. The results of the power spectral analysis for 850 mb v^* over the eastern Indian Ocean show marked spectral peaks between about 4 and 15 days (Fig. 9a). In contrast, results of the spectral analysis for v^{*2} are quite different (Fig. 9b). A pronounced spectral peak with a period of 30 days surpasses the 95% confidence level during the 1982–1983 winter. Similarly, spectral peaks with substantial power are seen in the 30–60 day period range during the 1979–1980 and 1980–1981 winters. This certainly confirms the presence of 30–60 day component in the v^{*2} variations which are associated with an amplitude modulation of synoptic-scale transient disturbances v^*. In short, the time scale of v^{*2} becomes much longer than that of individual transient disturbances v^*.

Having confirmed the low-frequency (30–60 day) mode in v^{*2}, we calculated eddy kinetic energy of transient disturbances, i.e., $k^* = (u^{*2} + v^{*2})/2$, at every grid point over the global domain. Then 30–60 day band-pass filter was applied to obtain $\tilde{k}^*$ time series at every grid point. The phase propagation of equatorial $\widetilde{OLR}$ perturbations is generally eastward (Fig. 6). Although individual transient disturbances (u^* and v^*) at 850 mb over the SH monsoon region propagate westward with a speed of about 5 m s^{-1}, lag correlation maps of $R(\tilde{\Phi}, \tilde{k}^*)$ confirm eastward propagation of $\tilde{k}^*$ (not shown). We also computed the simultaneous correlation between $\tilde{k}^*$ and $\tilde{\Phi}$, which is denoted as $r(\tilde{k}^*, \tilde{\Phi})$. In Fig. 10a, strong association of $\tilde{k}^*$ disturbance activity with low-frequency $\tilde{\Phi}$ oscillations can be noted over the subtropical and midlatitudes regions between 15° and 40° in both the NH and SH. Although individual transient disturbances have a small space scale (6000 km), a group of transient disturbances certainly has a planetary scale, and correlates well with the planetary-scale 30–60 day $\tilde{\Phi}$ perturbations. Namely, the space scale of $\tilde{k}^*$ becomes much larger than that of individual transient disturbances. Thus, these groups of transient disturbances may possibly interact and supply energy needed for the maintenance of the 30–60 day modes.

Fig. 10b depicts the zonally averaged correlation $\bar{r}(\tilde{k}^*, \tilde{\Phi})$. As mentioned before correlation is

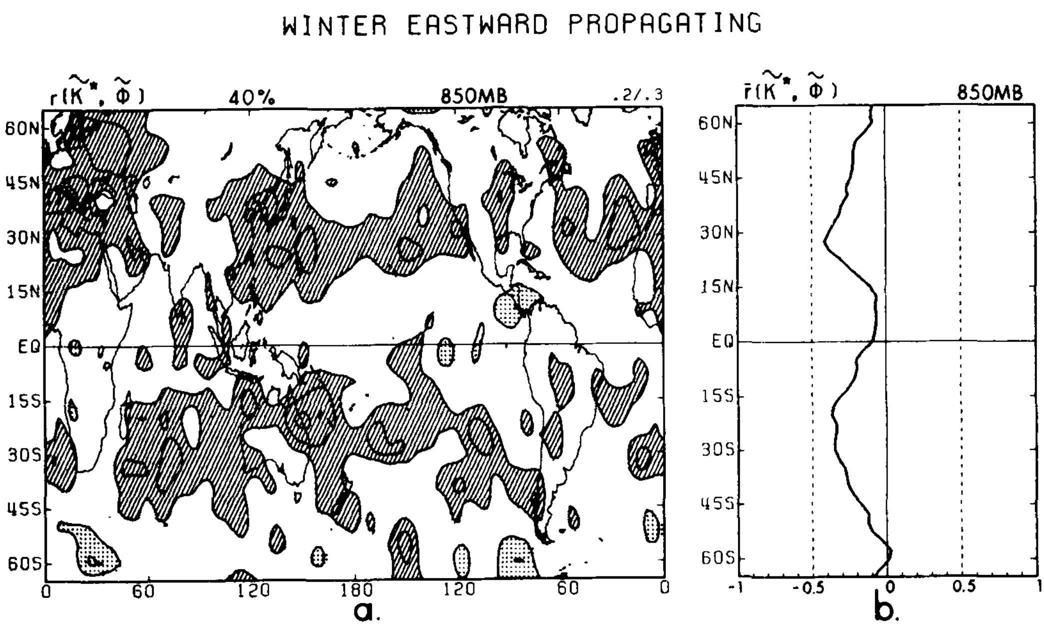

Fig. 10. (a) Simultaneous correlation between $\tilde{k}^*$ and $\tilde{\Phi}$ at 850 mb. Intervals are 0.2 and regions of correlation coefficient greater (less) than 0.3 (−0.3) are stippled (hatched). Also shown is the areal percentage that surpasses the local 95% confidence level of ±0.3. (b) Zonally average correlation.

less than -0.3 in the SH extratropics (15°–40°S) as well as the NH extratropics (20°–40°N). Near the equator, the zonal mean correlation is small, an indication of non-interactive nature of equatorial transient disturbances with 30–60 day oscillations. In this equatorial domain the low-frequency perturbations can be considered to be free modes, owing their existence to internally enhanced large-scale convections as theoretically predicted by Hayashi and Sumi (1986).

7. Conclusions

Using outgoing long-wave radiation (OLR), objectively analyzed daily winds (u, v) and geopotential height (Φ) data of 5 winters (1979–1984), space-time structure of low-frequency meridional flows of NH midlatitude origin and their relationship with tropical convection are investigated. In addition, the interaction between transient disturbances (perturbations with periods less than 30 days) and low-frequency (30–60 day) modes is examined.

The lag correlation maps for the transient component of 850 mb geopotential height display the regional character of low-level synoptic disturbances. Near Japan, these disturbances show an eastward phase speed of 10 m s^{-1} and a horizontal scale of about 6000 km. This reflects the nature of transient midlatitude baroclinic wave disturbances.

The correlation patterns of 30–60 day filtered 850 mb geopotential height show that these low-frequency modes are of global-scale character with zonal wavenumber one. The 30–60 day northerlies from Siberia lag behind the monsoon convection over the SH monsoon region (Indonesia–northern Australia–New Guinea) by about 10 days. Namely, the low-level northerly $\tilde{v}$ from Siberia does not contribute to the enhancement of 30–60 day equatorial convection. However, northeasterly $\tilde{v}$ of subtropical north Pacific origin, after crossing the equator, tends to intensify the monsoonal westerlies and the associated convective activity over the SH monsoon region.

The 200 mb correlation maps reveal strong upper-level southerly outflows $(\tilde{v} > 0)$ when the monsoon is active over Indonesia, northern Australia and New Guinea. These southerlies tend to accelerate the westerly jet $(\tilde{u} > 0)$ near Japan. The most important indication is that such active monsoon condition occurs approximately 10 days prior to the maximum low-level northerly $\tilde{v}$ from Siberia.

The transient component of meridional wind v^* off the west coast of Australia shows a typical periodicity around 4 to 15 days. These individual transient disturbances do not correlate with 30–60 day oscillations. However, v^{*2} indicate dominant spectral peaks in the 30–60 day period range. The space scale of v^{*2} becomes much larger than that of individual transient disturbances. Therefore, these transient disturbances, as a group, can correlate (interact) with 30–60 day planetary-scale perturbations. Interestingly, such nonlinear interaction appears to be most prominent in both the NH and SH extratropics (15°–40°). It is highly probable that extratropical 30–60 day perturbations are maintained, at least partially, through nonlinear interaction with transient disturbances.

As pointed out by Murakami et al. (1986), equatorial $\widetilde{OLR}$ perturbations are most pronounced near the maritime continent. Why is the activity of $\widetilde{OLR}$ perturbations unique to this particular region of the tropics? The present study presented evidence that this region is characterized by the occurrence of prominent equatorward $\tilde{v}$ winds, which eventually facilitate the development of equatorial low-frequency perturbations in winter. Similar features were also noted in summer (Murakami, 1987a). These features have important implications on the mechanisms of low-frequency oscillations as to whether they are forced and/or free atmospheric modes. In this regard, the most important conclusion in the present study is that they could be regarded as forced waves due primarily to equatorward $\tilde{v}$ winds (Sections 4, 5), and partially to the nonlinear interaction with transient synoptic disturbances (Section 6). This view is further supported by the fact that no significant low-level, midlatitude $\tilde{v}$ wind fluctuations occur during NE phase, when the activity of equatorial convection is depressed below normal (Fig. 1) and transient synoptic disturbances become weaker than usual (not shown).

8. Acknowledgements

The authors wish to thank Mrs. Dixie Zee for final editing of this manuscript. This research has been supported jointly by the National Science Foundation and the National Oceanic and Atmospheric Administration, Washington, DC, under the Research Grant ATM-8609968.

REFERENCES

Chang, C.-P. 1977. Viscous internal gravity waves and low-frequency oscillations in the tropics. *J. Atmos. Sci. 34*, 901–910.

Chang, C.-P. and Lau, K. M. 1982. Short-term planetary-scale interactions over the tropics and mid-latitudes during northern winter. Part I: Contrasts between active and inactive periods. *Mon. Wea. Rev. 110*, 933–946.

Gill, A. E. 1980. Some simple solutions for heat induced tropical circulations. *Q. J. R. Meteorol. Soc. 106*, 447–462.

Hayashi, Y. and Sumi, A. 1986. The 30–40 day oscillations in an "aqua planet" model. *J. Meteorol. Soc. Japan. 64*, 451–467.

Krishnamurti, T. N. and Gadgil, S. 1985. On the structure of the 30 to 50 day mode over the globe during FGGE. *Tellus 37*, 336–360.

Krishnamurti, T. N., Jayakumar, P. K., Sheng, J., Surgi, N. and Kumar, A. 1985. Divergent circulations on the 30–50 day time scale. *J. Atmos. Sci. 42*, 364–375.

Lau, K.-M. and Chen, P. H. 1985. Aspects of the 40–50 day oscillation during northern winter as inferred from outgoing longwave radiation. *Mon. Wea. Rev. 113*, 1889–1909.

Lau, K.-H. and Phillips, T. J. 1986. Coherent fluctuations of extratropical geopotential height and tropical convection in intraseasonal time scales. *J. Atmos. Sci. 43*, 1164–1181.

Lau, N.-G. and Lau, K.-M. 1986. The structure and propagation of intraseasonal oscillations appearing in a GFDL general circulation model. *J. Atmos. Sci. 43*, 2023–2047.

Lim, H. and Chang, C.-P. 1981. A theory for midlatitude forcing of tropical motions during winter monsoons. *J. Atmos. Sci. 38*, 2377–2392.

Lorenc, A. C. 1984. The evolution of planetary scale 200 mb divergence during the FGGE year. *Q. J. R. Meteorol. Soc. 110*, 427–441.

Madden, R. A. and Julian, P. R. 1971. Detection of a 40–50 day oscillation in the zonal wind in the tropical Pacific. *J. Atmos. Sci. 8*, 702–708.

Murakami, M. 1979. Large-scale aspects of deep convective activity over the GATE area. *Mon. Wea. Rev. 107*, 994–1013.

Murakami, T. 1987a. Intraseasonal atmospheric teleconnection pattern during the northern hemisphere summer. *Mon. Wea. Rev. 115*, 2133–2154.

Murakami, T. 1987b. Intraseasonal atmospheric teleconnection pattern during the northern hemisphere winter. *Mon. Wea. Rev. 115*, in press.

Murakami, T., Chen, L.-X., Xie, A. and Shrestha, 1986. Eastward propagation of 30–60 day perturbations as revealed from outgoing longwave radiation data. *J. Atmos. Sci. 43*, 961–971.

Quah, L.-C. 1984. On the 30–50 day tropospheric oscillation during the 1978–1979 northern winter. *J. Meteorol. Soc. Japan 62*, 261–272.

Ramage, C. S. 1971. *Monsoon meteorology*. Academic Press, 296 pp.

Ramage, C. S. 1984. Climate of the Indian Ocean north of 35°S. In *Climate of the oceans* (ed. H. van Loon). Elsevier, Amsterdam, pp. 603–671.

Shrestha, M. L. and Murakami, T. 1988. Intraseasonal fluctuation in low-level meridional winds over the Indian Ocean and monsoonal convection over South Asia. *Tellus 40*, 120–132.

Weickmann, K. M., Lussky, G. R. and Kutzbach, J. E. 1985. Intraseasonal (30–60 day) fluctuations of outgoing longwave radiation and 250 mb streamfunction during northern winter. *Mon. Wea. Rev. 113*, 941–961.